The generalized Wolf shift for cyclostationary fields

Robert W. Schoonover, Brynmor J. Davis, and P. Scott Carney

*Department. of Electrical and Computer Engineering and The Beckman Institute for
Advanced Science and Technology,
University of Illinois at Urbana-Champaign,
405 N. Mathews, Urbana, IL 61801, USA*

rschoono@uiuc.edu

Abstract: Correlation dependent, propagation-induced shifts in the generalized spectra of cyclostationary, random fields are predicted. This result generalizes the Wolf shift for stationary fields and is applicable to periodic trains of fast pulses such as might be generated in comb spectroscopy or other mode-locked pulsed systems. Examples illustrate these shifts for intrinsically stationary fields and the fields generated by a mode-locked laser.

© 2009 Optical Society of America

OCIS codes: (260.1960) Diffraction theory;(030.0030) Coherence and statistical optics; (320.7120) Ultrafast phenomena

References and links

1. E. Wolf, *Introduction to the Theory of Coherence and Polarization* (Cambridge University Press, 2007).
2. L. Mandel and E. Wolf, *Optical Coherence and Quantum Optics* (Cambridge University Press, 1995).
3. P. Corkum and Z. Chang, "The Attosecond Revolution," Opt. Photon. News **19**, 24–29 (2008).
4. W. Gardner, A. Napolitano, and L. Paura, "Cyclostationarity: Half a Century of Research," Signal Process. **86**, 639–697 (2006).
5. B. Davis, "Measurable Coherence Theory for Statistically Periodic Fields," Phys. Rev. A **76**, 043,843 (2007).
6. E. Wolf, "Invariance of the Spectrum of Light on Propagation," Phys. Rev. Lett. **56**, 1370–1372 (1986).
7. E. Wolf, "Noncosmological Redshifts of Spectral Lines," Nature (London) **326**, 363–365 (1987).
8. S. Ponomarenko, G. Agrawal, and E. Wolf, "Energy Spectrum of a Nonstationary Ensemble of Pulses," Opt. Lett. **29**, 394–396 (2004).
9. H. Lajunen, P. Vahimaa, and J. Tervo, "Theory of Spatially and Spectrally Partially Coherent Pulses," J. Opt. Soc. Am. A **22**, 1536–1545 (2005).
10. R. Gase and M. Schubert, "On the Determination of Spectral Properties of Non-stationary Radiation," J. Mod. Opt. **29**, 1331–1347 (1982).
11. R. Schoonover, B. Davis, R. Bartels, and P. Carney, "Optical Interferometry with Pulsed Fields," J. Mod. Opt. **55**, 1541–1556 (2008).
12. A. Kubo, K. Onda, H. Petek, Z. Sun, Y. Jung, and H. Kim, "Femtosecond Imaging of Surface Plasmon Dynamics in a Nanostructured Silver Film," Nano Lett **5**, 1123–1127 (2005).
13. Y. Liau, A. Unterreiner, Q. Chang, and N. Scherer, "Ultrafast Dephasing of Single Nanoparticles Studied by Two-pulse Second-order Interferometry," J. Phys. Chem. B **105**, 2135–2142 (2001).
14. T. Stievater, X. Li, D. Steel, D. Gammon, D. Katzer, D. Park, C. Piermarocchi, and L. Sham, "Rabi Oscillations of Excitons in Single Quantum Dots," Phys. Rev. Lett. **87**, 133,603 (2001).
15. J. Reichert, R. Holzwarth, T. Udem, and T. Hänsch, "Measuring the Frequency of Light with Mode-locked Lasers," Opt. Commun. **172**, 59–68 (1999).
16. D. Jones, S. Diddams, J. Ranka, A. Stentz, R. Windeler, J. Hall, and S. Cundiff, "Carrier-Envelope Phase Control of Femtosecond Mode-Locked Lasers and Direct Optical Frequency Synthesis," Science (London) **288**, 635 (2000).
17. B. Saleh and M. Teich, *Fundamentals of Photonics* (New York: Wiley-Interscience, 1991).
18. S. Jacobs, "The Optical Heterodyne," Electronics **36**, 29 (1963).
19. A. Siegman, S. Harris, and B. McMurtry, "Optical Heterodyning and Optical Demodulation at Microwave Frequencies," Optical Masers pp. 511–527 (1963).

20. T. Young, "The Bakerian Lecture. Experiments and Calculations Relative to Physical Optics," Phil. Trans. R. Soc. Lond **94** (1804).

1. Cyclostationary fields

The theory of statistically stationary optical fields, coherence theory [1, 2], provides a means to relate time-averaged measurements of optical intensities to the statistical properties of a scatterer or source. However, as ultrafast optical devices become more common and applications of short pulses become more wide-spread, it is clear that the theory of stationary fields alone is not sufficient to interpret measurements of optical fields or intensities [3]. A framework for analyzing physically realizable measurements from statistically periodic sequences of fast pulses based on the theory of cyclostationary processes [4] has recently been presented [5]. Cyclostationary signals differ from stationary signals in that the field may be correlated across distinct temporal frequencies. Thus the Wiener-Khintchine theorem [2] that defines the power spectrum must be generalized for cyclostationary processes, resulting in a sequence of generalized spectra. It has been shown that, for stationary optical sources, the power spectrum may undergo correlation-induced changes on propagation, the so-called Wolf shift [6, 7]. In this article, changes in the generalized power spectra and the two-frequency cross-spectral density are predicted for fields generated by cyclostationary sources.

Consider a stochastic, cyclostationary source $\sigma(\mathbf{r}, t)$ with mutual coherence function

$$\Gamma_\sigma(\mathbf{r}_1, \mathbf{r}_2, t - \tau, t) = \langle \sigma^*(\mathbf{r}_1, t - \tau)\sigma(\mathbf{r}_2, t) \rangle, \tag{1}$$

where the brackets denote an ensemble average. Cycloergodicity is assumed, so the appropriate ensemble averages and long time averages are equivalent. Cyclostationary processes exhibit a discrete time translation symmetry rather than the continuous symmetry of stationary processes, so $\Gamma(\mathbf{r}_1, \mathbf{r}_2, t - \tau, t) = \Gamma(\mathbf{r}_1, \mathbf{r}_2, t - \tau + T_0, t + T_0)$, *i.e.* the absolute time is only important modulo T_0. Because of this statistical periodicity, the mutual coherence function admits the Fourier series representation

$$\Gamma_\sigma(\mathbf{r}_1, \mathbf{r}_2, t - \tau, t) = \sum_{n=-\infty}^{\infty} C_n(\mathbf{r}_1, \mathbf{r}_2, \tau)e^{-i\omega_0 n t}, \tag{2}$$

where $\omega_0 = 2\pi/T_0$.

The Fourier transform of the mutual coherence function is the two-frequency cross-spectral density, viz.,

$$W_\sigma(\mathbf{r}_1, \mathbf{r}_2, \omega_1, \omega_2) = \int dt_1 dt_2 \, \Gamma_\sigma(\mathbf{r}_1, \mathbf{r}_2, t_1, t_2)e^{i(\omega_2 t_2 - \omega_1 t_1)}. \tag{3}$$

From Eq. (2) and Eq. (3), one finds that

$$W_\sigma(\mathbf{r}_1, \mathbf{r}_2, \omega, \omega + \Omega) = \sum_n \tilde{C}_n(\mathbf{r}_1, \mathbf{r}_2, \omega)\delta(\Omega - n\omega_0), \tag{4}$$

where $\tilde{C}_n$ is the Fourier transform of C_n. Equation (4) is a generalization of the Wiener-Khintchine theorem as may be seen by taking the $T_0 \to \infty$ ($\omega_0 \to 0$) limit. The $\tilde{C}_n(\mathbf{r}, \mathbf{r}, \omega)$ are generalized spectra and the $\tilde{C}_n(\mathbf{r}_1, \mathbf{r}_2, \omega)$ are generalized cross-spectra. In the usual form of the Wiener-Khintchine theorem, the delta function $\delta(\Omega)$ indicates that the field is uncorrelated across frequencies. In this generalized form, it is clear that the field is correlated only at discretely-spaced frequencies.

The measurement of the standard spectrum, where $\Omega = 0$, may be accomplished by means such as grating spectroscopy or Fourier transform spectroscopy. The spectral density of a source, secondary source, or field is given by the expression $S(\mathbf{r}, \omega) = W(\mathbf{r}, \mathbf{r}, \omega, \omega)$ [8], which implies that for cyclostationary fields the spectrum as would be measured in a standard spectrometer is given by the zeroth-order generalized spectra $S(\mathbf{r}, \omega) = \tilde{C}_0(\mathbf{r}, \mathbf{r}, \omega)$ [5]. In Sec. 2, the propagation laws for the cross-spectra are examined and the generalized Wolf shifts are identified. Examples are used to illustrate the Wolf shift for cyclostationary fields in Sec. 3. A scheme to measure the generalized spectra and cross-spectra by heterodyne techniques is proposed in Sec. 4.

2. Propagation of generalized cross-spectra

In general, the spectrum, or for cyclostationary processes, the generalized spectra, cannot be determined at arbitrary points from the known spectra of the source or even the spectra on some plane. Instead, it is necessary to propagate the two-point, and for nonstationary processes, two-frequency, cross-spectral density. It has been shown that the two-point, two-frequency cross-spectral density satisfies the Wolf equation [2, 9],

$$(\nabla_1^2 + k_1^2)(\nabla_2^2 + k_2^2)W_R(\mathbf{r}_1, \mathbf{r}_2, \omega, \omega + \Omega) = (4\pi)^2 W_\sigma(\mathbf{r}_1, \mathbf{r}_2, \omega, \omega + \Omega), \tag{5}$$

where W_σ is the source cross-spectral density and W_R is the cross-spectral density for the radiated field, $k_1 = \omega/c$ and $k_2 = (\omega + \Omega)/c$. The radiated field can thus be found by the method of Green functions, and the cross-spectral density for the radiated field in the far zone takes the form

$$W^{(\infty)}(\mathbf{r}_1, \mathbf{r}_2, \omega, \omega + \Omega) = \frac{e^{i(k_2 r_2 - k_1 r_1)}}{r_1 r_2} \mathscr{W}_\sigma(-k_1 \hat{r}_1, k_2 \hat{r}_2, \omega, \omega + \Omega), \tag{6}$$

where $\mathbf{r}_i = r_i \hat{r}_i$ and $\mathscr{W}_\sigma$ is the six-dimensional spatial Fourier transform of W_σ. For stationary fields [6], the peak of the spectrum of the radiated field generally shifts compared to the source spectrum as a direct consequence of the correlations in the source. From Eqs. (4) and (6) and using the sifting property of the δ-function, one obtains

$$W^{(\infty)}(\mathbf{r}_1, \mathbf{r}_2, \omega, \omega + \Omega) = \sum_n \frac{e^{i(k_{2,n} r_2 - k_1 r_1)}}{r_1 r_2} \mathscr{C}_n(-k_1 \hat{r}_1, k_{2,n} \hat{r}_2, \omega)$$
$$\times \delta(\Omega - n\omega_0), \tag{7}$$

where $k_{2,n} = (\omega + n\omega_0)/c$ and $\mathscr{C}_n$ is the six-dimensional spatial Fourier transform of $\tilde{C}_n$. Note that Eq. (7) is of the same form as Eq. (4), with $\tilde{C}_n(\mathbf{r}_1, \mathbf{r}_2, \omega) \rightarrow \exp(ik_{2,n}r_2 - ik_1 r_1)\tilde{\mathscr{C}}_n(-k_1\hat{r}_1, k_{2,n}\hat{r}_2, \omega)/(r_1 r_2)$. Because $\mathscr{C}_n$ and $k_{2,n}$ differ for each n, each generalized spectrum may experience a different spectral shift. Thus the standard Wolf shift may be seen in $\tilde{C}_0$, and a sequence of generalized Wolf shifts may be seen in each of these generalized spectra. This is the main result of this article, which is illustrated below through example.

The measured spectrum in the far zone is given by

$$S^{(\infty)}(\mathbf{r}, \omega) = \frac{\tilde{\mathscr{C}}_0(-k\hat{r}, k\hat{r}, \omega)}{r^2}. \tag{8}$$

Equation (8) is of the same form as the propagation rule for the spectrum in the stationary case [2], where $\tilde{\mathscr{C}}_0$ takes the place of the one-frequency cross-spectral density. There is no equivalent expression for the propagation rule for the generalized spectra in the theory of stationary fields. It is also important to note that all of the generalized spectra contribute to the optical intensity $I(\mathbf{r}, t) = \Gamma(\mathbf{r}, \mathbf{r}, t, t)$, and thus the propagated pulse shape.

3. Examples

As a model for a cyclostationary field, consider a stationary source with mutual coherence function $\bar{\Gamma}(\mathbf{r}_1, \mathbf{r}_2, \tau)$ that is modulated periodically in time with period T_0. Such a field is called intrinsically stationary [10, 11]. Let the periodic modulation function be given by $h(t)$ with period T_0. The Fourier transform of the underlying stationary mutual coherence function is the single frequency cross-spectral density,

$$\bar{W}(\mathbf{r}_1, \mathbf{r}_2, \omega) = \int d\tau \, \bar{\Gamma}(\mathbf{r}_1, \mathbf{r}_2, \tau) e^{i\omega\tau}. \tag{9}$$

The modulation function has a Fourier representation $h(t) = \sum_n h_n \exp(-i\omega_0 n t)$, where $\omega_0 = 2\pi/T_0$. After modulation, the source has a two-time mutual coherence function, $\Gamma(\mathbf{r}_1, \mathbf{r}_2, t - \tau, t) = \bar{\Gamma}(\mathbf{r}_1, \mathbf{r}_2, \tau)h(t)h^*(t - \tau)$. Inserting this expression for the mutual coherence function into Eq. (3) and using Eq. (8), the measured spectrum in the far zone is found to be

$$S^{(\infty)}(\mathbf{r}, \omega) = \frac{1}{r^2} \sum_n |h_n|^2 \mathscr{\bar{W}}(-k\hat{r}, k\hat{r}, \omega - n\omega_0), \tag{10}$$

where $\bar{\mathscr{W}}$ is the six-dimensional Fourier transform of the stationary cross-spectral density of the source $\bar{W}$ and $k = \omega/c$. The modulation and the propagation both affect the spectrum in the far zone in a complicated manner for a general source. When the source can be factorized $\bar{W}(\mathbf{r}_1, \mathbf{r}_2, \omega) = A(\omega)D(\mathbf{r}_1, \mathbf{r}_2)$, the effects of modulation and propagation can be separated:

$$S^{(\infty)}(\mathbf{r}, \omega) = \frac{\tilde{\mathscr{D}}(-k\hat{r}, k\hat{r})}{r^2} \sum_n |h_n|^2 A(\omega - n\omega_0). \tag{11}$$

The original spectrum, A, is broadened by the modulation, and then shifted in the course of propagation as a result of the factor $\tilde{\mathscr{D}}$.

As an example, consider a collection of M point-sources that are identically modulated. The source density for this system is given by the expression

$$\sigma(\mathbf{r}, t) = \sum_{n=-\infty}^{\infty} \sum_{p=1}^{M} \sigma_p(t) h_n \exp(-in\omega_0 t) \delta^{(3)}(\mathbf{r} - \mathbf{r}^{(p)}), \tag{12}$$

where $\sigma_p(t)$ is the source density at point $\mathbf{r}^{(p)}$. The underlying sources, σ_p, are assumed to be partially correlated, stationary, random processes. The frequency-domain correlation function for the $\{\sigma_p\}$ is written

$$\langle \tilde{\sigma}_p^*(\omega) \tilde{\sigma}_q(\omega') \rangle = S(\omega) \mu_{pq}(\omega) \delta(\omega - \omega'), \tag{13}$$

where $\langle \cdot \rangle$ denotes an ensemble average and μ_{pq} is the spectral degree of coherence between the point sources at $\mathbf{r}^{(p)}$ and $\mathbf{r}^{(q)}$, respectively. Each point source is taken to have the same spectrum, $S(\omega)$. The field radiated from the collection of modulated sources has a two-frequency cross-spectral density

$$W^{(\infty)}(\mathbf{r}_1, \mathbf{r}_2, \omega, \omega + \Omega) = \sum_{m,n} \sum_{p,q=1}^{M} h_n^* h_{m+n} \frac{e^{-ik_1|\mathbf{r}_1 - \mathbf{r}^{(p)}|}}{|\mathbf{r}_1 - \mathbf{r}^{(p)}|} \frac{e^{ik_{2,m}|\mathbf{r}_2 - \mathbf{r}^{(q)}|}}{|\mathbf{r}_2 - \mathbf{r}^{(q)}|}$$
$$\times S(\omega - n\omega_0) \mu_{pq}(\omega - n\omega_0) \delta(\Omega - m\omega_0). \tag{14}$$

In Fig. 1 the normalized spectra, $\tilde{C}_0$ and $|\tilde{C}_4|$, are shown at both the sources and at a point far away for a collection of three sources, located along the x-axis at $x = 100$ mm, $x = 0$ mm, and $x = -100$ mm, respectively. The $\{h_n\}$ represent a square wave with a 10% duty cycle, $S(\omega)$ is taken to be a Gaussian function with 20% bandwidth and center frequency $\omega_c = 5 \times 10^{15}$ rad/s, and the spectral degree of coherence is taken to be

$$\mu_{ij}(\omega) = \begin{cases} 1 & i = j \\ \mu \exp\left(-\frac{(\omega - \omega_c)^2}{2\chi^2}\right) & i \neq j, \end{cases} \tag{15}$$

where χ is the bandwidth of the coherence function, assumed to be the bandwidth of the spectrum for this example. In the top two panels, the normalized generalized spectra for $\tilde{C}_0$ and $|C_4|$ are shown for sources that are highly correlated ($\mu = 0.8$). The middle two panels show simulations of the same system as in the top two panels, except that the sources are less correlated ($\mu = 0.1$). The peak frequency for both $\tilde{C}_0(\omega)$ and $|\tilde{C}_4(\omega)|$ are each less red-shifted in the lower-coherence case. In the bottom panels of Fig. 1, $\tilde{C}_0$ and $|C_4|$ are shown for the same system as in the middle two panels, except that the repetition rate of the system has been changed from 1% of the center frequency to 5% of the center frequency. In this case, the length of the pulse is two optical cycles. Note that while the plot for $\tilde{C}_0$ is only slightly changed on propagation at the higher repetition rate, the plot for $\tilde{C}_4$ is much changed, with the secondary peak red-shifted instead of blue-shifted from the primary peak.

The example above may be realized in experiments in which a partially spatially coherent, cyclostationary, optical field illuminates small, point-like objects, for example in imaging of nanoparticles and quantum dots [12, 13, 14]. The objects are then secondary sources, and the field scattered from those objects can exhibit shifts in the generalized spectra.
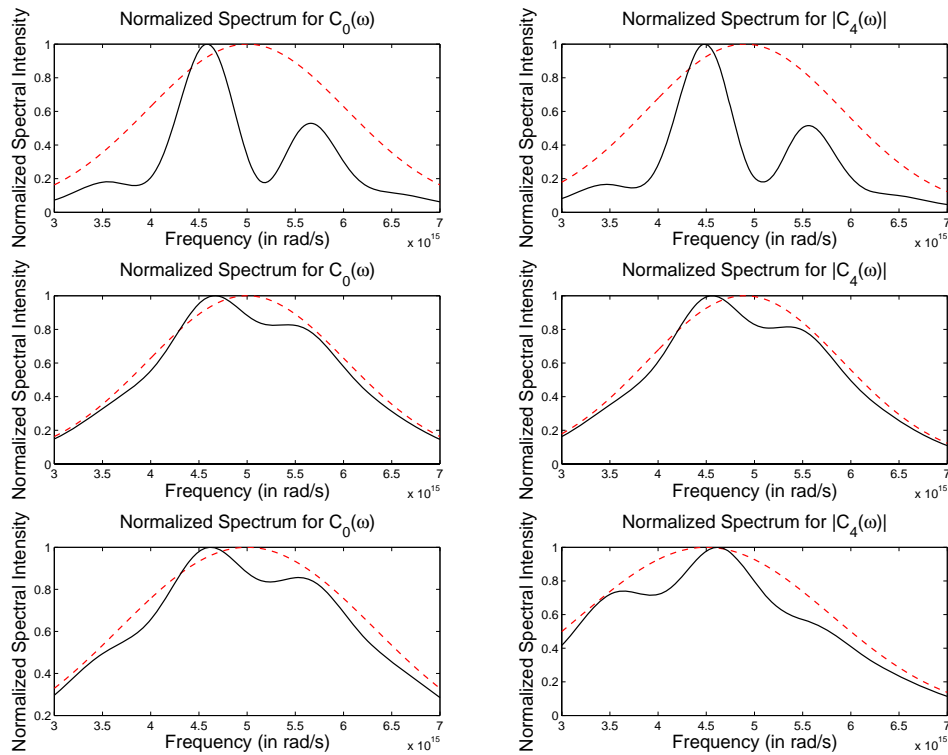
Fig. 1. (Color online) The normalized spectral density $\tilde{C}_0(\omega)$ and the spectral correlation function $|\tilde{C}_4(\omega)|$ normalized by its peak, at the source (dashed lines in red) and at a point in the far zone $P = (100, 0, 12000)$ mm (shown in black) for the case when there are three sources, located at (-100,0,0) mm, (0,0,0) mm, and (100,0,0) mm. The peak of $\tilde{C}_0(\omega)$ is at a higher frequency than the peak of $|\tilde{C}_4(\omega)|$. The top two panels contain plots of $\tilde{C}_0$ and $|\tilde{C}_4|$ for a three-source system with $\mu = 0.8$, the repetition frequency is taken to be 5×10^{13} rad/s, the bandwidth of the coherence and the bandwidth of the spectrum are both 20% of the center frequency $\omega_c = 5 \times 10^{15}$ rad/s. The middle two panels contain plots of $\tilde{C}_0$ and $|\tilde{C}_4|$ for the same three-source system as above, only with $\mu = 0.1$. The bottom two panels contain plots of $\tilde{C}_0$ and $|\tilde{C}_4|$ for a three-source system that differs from the one in the middle panels by changing the repetition frequency from 5×10^{13} rad/s to 2.5×10^{14} rad/s.

As another model for the generation of cyclostationary light, consider a mode-locked laser in which the carrier envelope has phase fluctuations. The electric field at the output of a mode-locked laser can be modeled by $U(\mathbf{r},t) = f(\mathbf{r})\sum_n A_n \exp[i(\omega_c + n\omega_0)t]$ [15], where $\{A_n\}$ describe the periodic envelope around the carrier wave centered at ω_c. While in the idealized case the phase between the carrier wave and the envelope can be perfectly matched [16], in reality, there is some random phase between the output comb lines. The $\{A_n\}$ are random coefficients with correlation matrix $\alpha_{nm} = \langle A_n^* A_m \rangle$. The two-frequency cross-spectral density at the output plane can be put in the form of Eq. (4) with

$$\tilde{C}_m(\mathbf{r}_1,\mathbf{r}_2,\omega) = F(\mathbf{r}_1,\mathbf{r}_2)\sum_n \alpha_{nn+m}\delta(\omega - \omega_c + n\omega_0) \tag{16}$$

and $F(\mathbf{r}_1,\mathbf{r}_2) = f^*(\mathbf{r}_1)f(\mathbf{r}_2)$. If the phase fluctuations at the output plane are depend on position, the function $F(\mathbf{r}_1,\mathbf{r}_2)$ will not be separable and the source will be spatially partially coherent. The field that propagates away from the output plane will then exhibit the correlation-induced shifts presented in this article.

4. Detection of the generalized cross-correlation functions

Interferometric measurements are often made to determine the statistical properties of stationary fields. Because of the increase in the dimensionality in the case of cyclostationary fields (two time variables instead of one), conventional interferometric measurements must be augmented in some manner to make possible the inference of the statistical properties of the field [5]. For a cyclostationary field with correlation function $\Gamma(\boldsymbol{\rho}_1,\boldsymbol{\rho}_2,t-\tau,t) = \sum_m C_m(\boldsymbol{\rho}_1,\boldsymbol{\rho}_2,\tau)\exp(-im\omega_0 t)$ at the plane $z=0$ of a Sagnac or Mach-Zehnder interferometer [17, see Ch. 2], the intensity at the output of the interferometer is given by the expression

$$
\begin{aligned}
I(\boldsymbol{\rho},t;\tau) \propto\ & C_0(\boldsymbol{\rho},\boldsymbol{\rho},0) + |C_0(\boldsymbol{\rho},\boldsymbol{\rho},\tau)|\cos\alpha_0(\boldsymbol{\rho},\tau) \\
+\ & 2\sum_{m=1}^{\infty}\left\{|C_m(\boldsymbol{\rho},\boldsymbol{\rho},0)|\cos\left(\frac{m\omega_0\tau}{2}\right)\cos[m\omega_0(t-\tau/2)-\alpha_m(\boldsymbol{\rho},0)]\right. \\
+\ & |C_m(\boldsymbol{\rho},\boldsymbol{\rho},\tau)|\cos[m\omega_0 t - \alpha_m(\boldsymbol{\rho},\tau)] + |C_{-m}(\boldsymbol{\rho},\boldsymbol{\rho},\tau)|\cos[m\omega_0 t + \alpha_{-m}(\boldsymbol{\rho},\tau)]\Big\},
\end{aligned}
\tag{17}
$$

where $\boldsymbol{\rho}$ is the planar coordinate on the detector, $\alpha_m(\boldsymbol{\rho},\tau) = \arg[C_m(\boldsymbol{\rho},\boldsymbol{\rho},\tau)]$ and τ is the delay in one of the interferometer arms. Since the time dependence is purely sinusoidal, a heterodyne detection scheme [18, 19] at the output of the interferometer allows each term in the sum in Eq. (17) to be determined individually. In heterodyne detection, the electrical signal from a detector is mixed with a sinusoidal electrical signal (the local oscillator). The output of a heterodyne detector is the amplitude of the original signal at the frequency of the local oscillator. The local oscillator frequency may be tuned to values $m\omega_0 = 2\pi m/T_0$ to obtain each term in Eq. (17) separately.

At the observation plane of a Young's two-pinhole interferometer [20], the measured intensity of an incident cyclostationary field is given by the expression

$$
\begin{aligned}
I_{12}(t;\tau) \propto\ & C_0^{(11)}(0) + C_0^{(22)}(0) + 2\left|C_0^{(12)}(\tau)\right|\cos\left[\alpha_0^{(12)}(\tau)\right] \\
+\ & 2\sum_{m=1}^{\infty}\left\{|C_m^{(11)}(0)|\cos[m\omega_0(t-R_1/c)+\alpha_m^{(11)}(0)]\right. \\
+\ & |C_m^{(22)}(0)|\cos[m\omega_0(t-R_2/c)+\alpha_m^{(22)}(0)] \\
+\ & |C_m^{(12)}(\tau)|\cos[m\omega_0(t-R_2/c)+\alpha_m^{(12)}(\tau)] \\
+\ & |C_m^{(21)}(-\tau)|\cos[m\omega_0(t-R_1/c)+\alpha_m^{(21)}(-\tau)]\Big\},
\end{aligned}
\tag{18}
$$

where $C_m^{(ij)}(\tau) = C_m(P_i,P_j,\tau)$, P_i is the location of the pinhole i, $\alpha_m^{(ij)}(\tau) = \arg[C_m^{(ij)}(\tau)]$ and $\tau = (R_1 - R_2)/c$, with R_i being the distance between the pinhole located at P_i. Again, a heterodyne detection scheme will yield each term in the sum in Eq. (18) individually. By varying the locations of the pinholes, the generalized correlation functions C_m may be recovered.

The correlation induced changes in the field upon propagation are observable in the detection scheme described above. Suppose the field with correlation function $\Gamma(\boldsymbol{\rho},\boldsymbol{\rho},t-\tau,t) = \sum_m C_m(\boldsymbol{\rho},\boldsymbol{\rho},\tau)\exp(-im\omega_0 t)$ on a plane $z = 0$ is allowed to propagate to a plane $z = z', z' \gg 0$ where another Mach-Zahnder interferometer is present. The intensity at the output of the interferometer is given by

$$
\begin{aligned}
r^2 I(\boldsymbol{\rho},t;\tau) \quad \propto \quad & F_0(\hat{r},0) + |F_0(\hat{r},\tau)|\cos\phi_0(\hat{r},\tau) \quad\quad\quad\quad\quad\quad\quad\quad\quad\quad\quad (19)\\
+ \quad & 2\sum_{m=1}^{\infty}\left\{|F_m(\hat{r},0)|\cos\left(\frac{m\omega_0\tau}{2}\right)\cos[m\omega_0(t-\tau/2-r/c)-\phi_m(\hat{r},0)]\right.\\
+ \quad & |F_m(\hat{r},\tau)|\cos[m\omega_0(t-r/c)-\phi_m(\hat{r},\tau)]\\
+ \quad & \left. |F_{-m}(\hat{r},\tau)\cos[m\omega_0(t-r/c)+\phi_{-m}(\hat{r},\tau)]\right\}
\end{aligned}
$$

where $F_m(\hat{r},\tau) = \frac{1}{2\pi}\int\tilde{\mathscr{C}}_m(-k_1\hat{r},k_{2,m}\hat{r},\omega)\exp(-i\omega\tau)\mathrm{d}\omega$, $\phi_m(\hat{r},\tau) = \arg[F_m(\hat{r},\tau)]$, r is the distance between the detector and the source, and the mapping between $\hat{r}$ and $\boldsymbol{\rho}$ is $\boldsymbol{\rho}/r = \hat{r}_\perp$. Heterodyne detection can then be used to find each term in the sum. The coherence-induced changes in the field can then be determined by comparison of the terms at frequency $m\omega_0$ at the planes $z = 0$ and $z = z'$.

In this article, it has been shown that the Wolf shift from the theory of stationary, partially-coherent fields, can be seen as well in fields governed by the theory of cyclostationary, partially coherent random processes. In this more general setting, a new set of phenomena are predicted: distinct generalized Wolf shifts for each of the generalized spectra. The spectral correlation functions for cyclostationary fields, each representing a correlation between distinct frequencies, undergo separate shifts based on the repetition frequency of the system and the spatial properties of the source. These correlation-dependent, propagation-induced shifts will each contribute separately to changes in the measured intensity of the field far from the source, and may be seen individually in a combined interferometric-heterodyne detection scheme.

Acknowledgments